



ISTITUTO NAZIONALE DI GEOFISICA E VULCANOLOGIA

**ACCEPTED ON ANNALS OF GEOPHYSICS, 61, 2018; Doi:
10.4401/ag-8048**

Understanding Basaltic Lava Flow Morphologies and Structures for Hazard Assessment

Sonia Calvari

**Istituto Nazionale di Geofisica e Vulcanologia, Osservatorio Etneo - Sezione di
Catania Piazza Roma 2, 95125 Catania (Italy)**

1 **Understanding Basaltic Lava Flow Morphologies and Structures for Hazard**

2 **Assessment**

3
4 Sonia Calvari

5 Istituto Nazionale di Geofisica e Vulcanologia, Osservatorio Etneo - Sezione di Catania

6 Piazza Roma 2, 95125 Catania (Italy)

7 Contact email: sonia.calvari@ingv.it; tel. +39 095 7165862

8 **Annals of Geophysics, 2019, in print**

9 10 **Abstract**

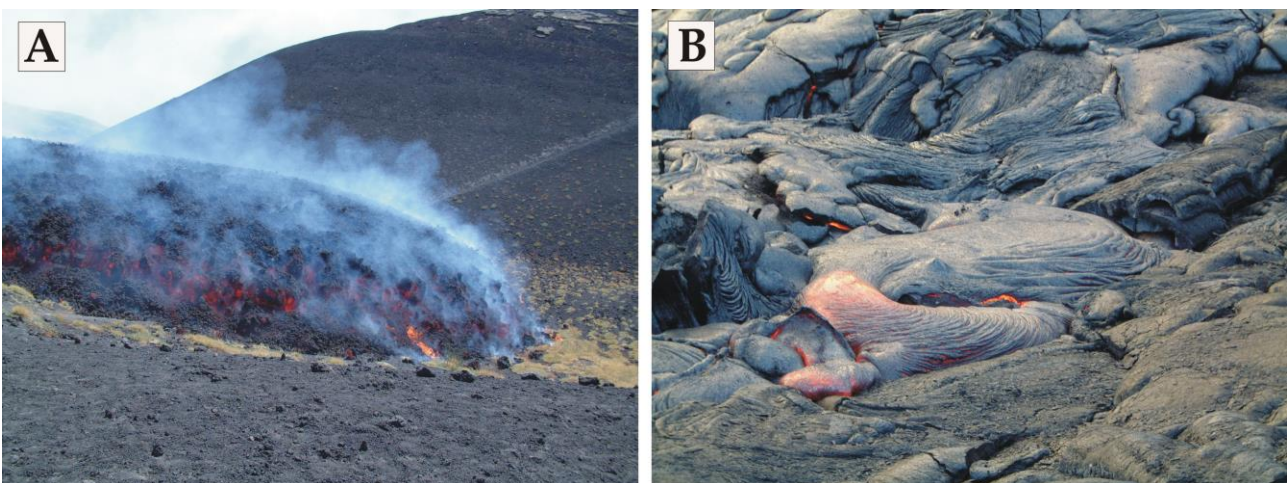
11 Lava flow surface morphologies are like pages of a book. If we are able to read the writing of that
12 book, we can understand its content, and learn, act, and react accordingly. In the same way, if we
13 understand lava surface morphology, recognise how it formed and the hazard it poses while
14 flowing, we can adopt actions to protect from lava flow invasion our villages, infrastructures and
15 local population. The surface of lava is a function of intrinsic and extrinsic qualities, and their
16 combination results in different shapes, sizes, and complexities, as well as in different hazards.
17 Initial sheet flows spreading at high speed have great potential for devastating land, as happened
18 in Hawaii in May-August 2018 (Neal et al., 2018). However, their destructive potential
19 significantly decreases with time and distance from the vent. Conversely, lava oozing from the
20 distal exit of lava tubes moves slowly but allows the tubes to expand, increasing gradually and
21 slowly the potential hazard for invasion of more remote lands. In this paper, I present an overview
22 of diverse lava flow surfaces, morphologies and structures in a framework of their generating
23 eruptive parameters, in order to suggest preliminary but prompt hazard evaluations that could be
24 applied during the initial phases of effusive volcanic crises at basaltic volcanoes worldwide.

25 26 **1. Introduction**

27 The final morphology of a solidified lava flow is the result of complex interactions between the
28 lava and the environment in which it is emplaced. Lava flows display several shapes, sizes and
29 surface morphologies, mainly determined by the physical and chemical properties of the lava, its
30 temperature, rate of effusion, crystal and gas content, but also by the local conditions such as
31 gravitational field strength and topography (Peterson & Tilling, 1980; Kilburn & Guest, 1993;

32 Harris et al., 2017a, 2017b). The main parameter influencing the morphology of a lava flow is its
33 non-Newtonian rheology, which causes the lava to rest on a slope, although unconfined by
34 topography, as soon as the supply ceases (Hulme, 1974). In turn, lava rheology depends on its
35 composition, temperature, crystal and gas contents (Giordano & Russell, 2018). The second most
36 important parameter influencing lava flow morphology is the rate of effusion (Walker, 1971),
37 which defines the maximum length that a channelized lava flow can attain (Walker, 1973).
38 Morphologies of solidified basaltic lava flows can be broadly divided into two categories: (i) aa or
39 (ii) pahoehoe, whereas the term “block lava” is generally used for thick brecciated lavas that are
40 typically more silicic than basalt (Harris et al., 2017a, 2017b), and thus is not considered here. Aa is
41 the type of lava that in solidified form is characterized by a rough, jagged, spiny and generally
42 clinkery surface (Figure 1A). Conversely, pahoehoe lava displays a smooth, billowy, or ropy
43 surface and normally comprises interconnected multiple flow lobes (Figure 1B). Harris et al.
44 (2017b) offer a comprehensive review of all terms used to define lava flow morphology, describing
45 also the many different varieties of pahoehoe and aa recognised in volcanology. For the aim of this
46 paper, which is essentially to characterize lava flows in order to reveal their hazard, I consider
47 only the two basic types, aa and pahoehoe. It is here worth noting that aa lava flows generally
48 advance faster than pahoehoe, and therefore pose a greater hazard (Kauahikaua & Tilling, 2014).
49 Thus, a greater attention will be devoted to the emplacement of the faster and more hazardous aa
50 lava flows.

51



52

53 **Figure 1** - (A) Expanding aa lava flow front at Mount Etna (Italy), 18 July 2001. The width of the image is
54 about 15 m. Photo by INGV. (B) Expanding pahoehoe flow lobes at Kilauea volcano (Hawaii). The width of
55 the image is about 3 m.

56

57 Most Hawaiian lavas initially erupt as pahoehoe, and may change to aa downstream as they flow
58 away from the vent (Peterson & Tilling, 1980; Lipman & Banks, 1987; Cashman et al., 1999). This
59 transition is caused by cooling and by increase in viscosity and yield strength during flowage
60 (Kilburn, 1981). At Etna, Stromboli and Fogo volcanoes instead, aa lavas are the most common
61 surface morphology among early lava flows, with pahoehoe becoming more widespread later in
62 an eruption when effusion rate declines (Calvari et al., 1994, 2005, 2018; Calvari & Pinkerton, 1998;
63 Lodato et al., 2007). Although pahoehoe and aa can be part of the same lava flow, they differ for
64 temperature, viscosity, and vesicles shapes, with most active pahoehoe flows being less viscous
65 and erupted at higher temperature than aa flows, and having vesicles normally as regular
66 spheroids (Peterson & Tilling, 1980). Conversely, aa flows have vesicles that tend to be irregularly
67 shaped, as a result of the deformation caused by movement during the final stages of solidification
68 (Peterson & Tilling, 1980). Even though aa lava tends to be more viscous, molten lava of
69 approximately the same initial viscosity may form either pahoehoe or aa, with the transition from
70 one to the second determined by a balance between viscosity and motion. Thus, in addition to the
71 effect of increasing viscosity, lava tends to change into aa also when subjected to flow turbulence
72 and internal shearing, such as during vigorous fountaining, pouring down steep slopes or
73 prolonged flowage for great distances (Peterson & Tilling, 1980).

74

75 Pahoehoe and aa lavas have different modalities of emplacement. Pahoehoe starts as small lobes
76 inflating to form wide and thick sheet flows several times greater than initial flow lobes (Figure 1B;
77 Hon et al., 1994; Keszthelyi & Denlinger, 1996; Harris et al., 2007b). Conversely, aa lavas move as a
78 caterpillar, producing an accumulation of clinkers in the front zone overrun by fluid lava, thus
79 forming a sort of sandwich with clinkers above and below and a fluid compact lava in between
80 (Figure 1A). Aa lavas move by pulses and display significant variations of the magma flux, with
81 pulses of increased flux in the front region considered as the distal result of more frequent flux
82 changes in the vent region (Bailey et al., 2006; James et al., 2007; Favalli et al., 2010). Pahoehoe
83 flows also expand intermittently, with alternating phases of lobes inflation and frontal expansion
84 (Hon et al., 1994). As with pahoehoe, aa lava flows are prone to inflate, forming extensive and
85 complex lava tubes, although this process is more difficult to detect than in pahoehoe flows
86 (Calvari & Pinkerton, 1998; James et al., 2009). At Etna volcano, pulses during the expansion of aa
87 lava flows (Lautze et al., 2004; Bailey et al., 2006; James et al., 2007, 2010, 2012; Favalli et al., 2010)

88 generate characteristic surface morphologies, influence volume distribution around the lava flow
 89 field, and construct the distal, medial and proximal channel segments (Favalli et al., 2010).

90

91 The largest historic basaltic lava flow field is probably that formed in Iceland during the 1783-1784
 92 Laki eruption, when 14.7 km³ of lava erupted at initial instantaneous effusion rate (IER) of up to
 93 $8.7 \times 10^3 \text{ m}^3 \text{ s}^{-1}$, forming in 8 months ~600 km² of a mostly pahoehoe lava flow field (Thordarson &
 94 Self, 1993; Guilbaud et al., 2005). Lava flow speed during the initial phases of that eruption was up
 95 to 15-17 km/day (Table 1; Thordarson & Self, 1993). The lava flow field initially emplaced as thin
 96 pahoehoe lobes that gradually coalesced into larger sheet lobes (Guilbaud et al., 2005), an
 97 expansion similar to most pahoehoe lava flow fields observed today on Kilauea (Hon et al., 1994;
 98 Kauahikaua et al., 1998; Patrick et al., 2017).

99

Lava type	Volcano	Eruption	Peak TADR (m ³ s ⁻¹)	Flow front velocity, reported	Flow front velocity m s ⁻¹	Reference
Aa sheet flow	O Shima (Japan)	1951		50 km/h	13.889	Mason & Foster, 1953
Aa sheet flow	Etna (Italy)	1991-93		2 km/day	0.023	Calvari et al., 1994
Channelized aa lava flows	Piton de la Fournaise, (La Réunion)	Dec 2010	38		7.30	Soldati et al., 2018
Channelized aa lava flows	Holuhraun (Iceland)	2014-15	350	1.13 km/day	0.131	Pedersen et al., 2017
Channelized aa flows	Mauna Loa (Hawaii)	1984	806			Lipman & Banks, 1987
Channelized aa flows	Etna (Italy)	May 2001	0.7	0.29 m/s	0.29	Bailey et al., 2006
Channelized aa flows	Etna (Italy)	1981	640		1.67 0.56	Guest et al., 1987 Coltelli et al., 2012
Channelized aa flows	Etna (Italy)	1983	50		0.02	Guest et al., 1987
Aa flow front	Mauna Loa (Hawaii)	1950	1,179-1,769	5.8 miles/h	2.59	Finch & Macdonald, 1953
Aa flow front	Etna (Italy)	2006		5 m/h	5.00	Favalli et al., 2010
Pahoehoe sheet flow	Kilauea (Hawaii)	2014-15		400-500 m/day	0.006	Poland et al., 2016; Patrick et al., 2017
Pahoehoe sheet flow	Kilauea (Hawaii)	23 Jan 1988	1.1	150 m/1.25 h	0.029	Hon et al., 1994
Pahoehoe flow	Kilauea (Hawaii)	1960	58-116	30 km/h	8.333	Macdonald 1962
Pahoehoe	Laki (Iceland)	1783-84	8,700	15-17 km/day	0.17-0.20	Thordarson & Self, 1993; Guilbaud et al., 2005

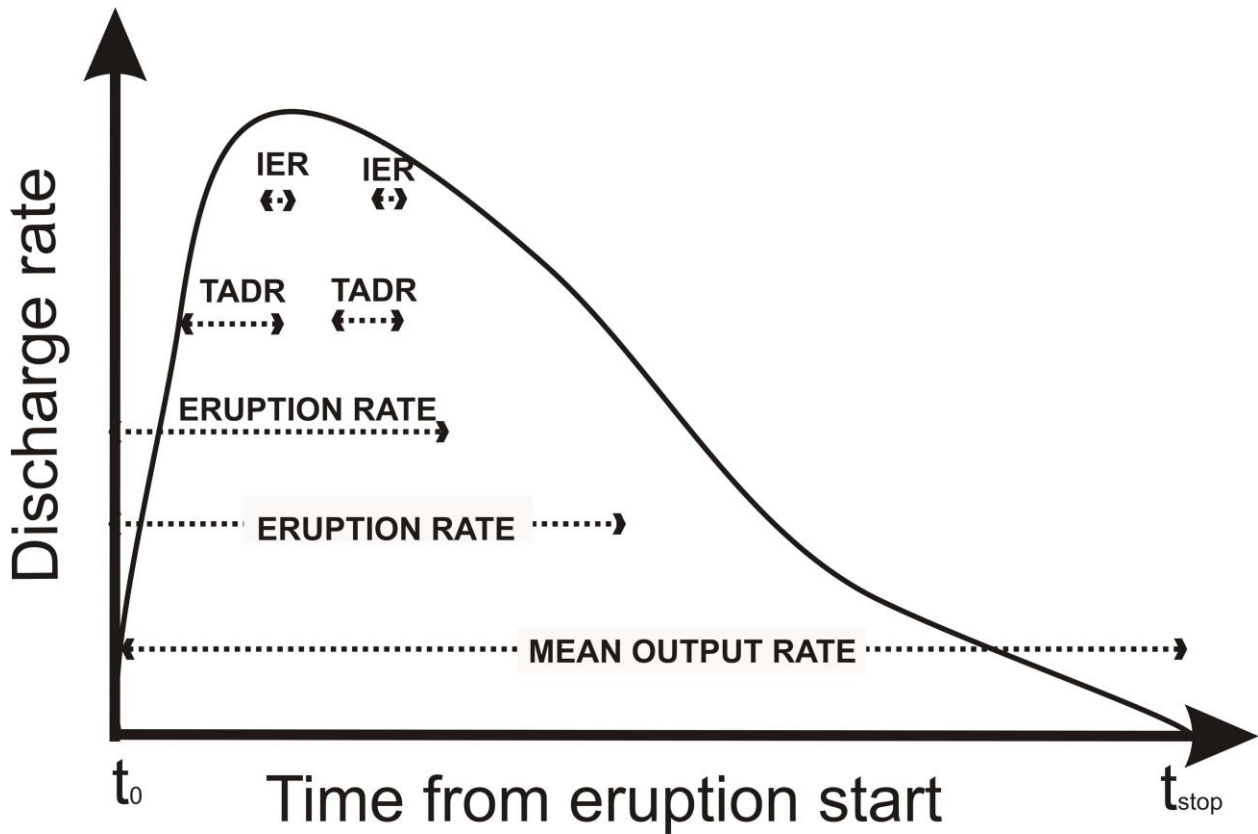
100 **Table 1** - Peak values of lava flows emplacement rates (TADR = time-averaged discharge rate) as a function
 101 of their surface morphology.
 102

103 At basaltic volcanoes like Etna and Stromboli (Italy), Kilauea (Hawaii), Piton de la Fournaise (La
104 Réunion), Fogo (Cape Verde), or Holuhraun (Iceland), the general shape of a complex lava flow
105 field is defined by a few arterial lava flows generally displaying aa texture, with its outline
106 modified by secondary lava flows normally having a pahoehoe surface (Guest et al., 1987; Kilburn
107 & Lopes, 1988, 1991; Calvari et al., 2005, 2018; Rhéty et al., 2017; Pedersen et al., 2017). When lava
108 tubes develop within complex lava flows, their hidden path is revealed by the distribution of
109 skylights, ephemeral vents or breakouts, tumuli, shatter rings, or pressure ridges (Guest et al.,
110 1980; Mattox et al., 1993; Calvari & Pinkerton, 1998; Kauahikaua et al., 1998, 2003; Calvari et al.,
111 1994, 2018). The formation of lava tubes significantly increases the hazard posed by an expanding
112 lava flow because their insulating effect allows the flow to spread further down slope. In the
113 following sections, I will give a brief introduction of the terms used to describe the effusion rate
114 when calculated on different time spans, and then describe the modalities of emplacement of lava
115 flows and flow fields, their structures and speed of formation considering several examples
116 worldwide, in order to assess their potential hazard and suggest how to organize risk mitigation.

117

118 2. TADR, ER, IER

119 Harris et al. (2007a; 2017a) present a review of effusion rate definitions (Figure 2), here
120 summarised to have clear in mind the time scale and size of the phenomena that I am considering.
121 Following Harris et al. (2007a, 2017a), I use instantaneous effusion rate (IER) for the volume flux of
122 erupted lava that is feeding a flow at any particular point in time; time-averaged discharge rate
123 (TADR) for the volume fluxes over a given time period (e.g., monthly, weekly, daily); eruption rate
124 (ER) for the total volume of lava emplaced since the beginning of the eruption divided by the time
125 since the eruption began; and mean output rate (MOR) for the final volume of erupted lava
126 divided by the total duration of the eruption, which can be obtained only once that the eruption is
127 over (Figure 2). Dense Rock Equivalent (DRE) standard is desirable when comparing available
128 data because it is independent from vesicle content, but past data and those collected from ground
129 measurements rather than from satellite often fail to mention if the volume is expressed as bulk
130 (including vesicles) or DRE (excluding vesicles). This is the case of most of the data in Table 1.



131

132 **Figure 2** - Scheme modified after Harris et al. (2007a), showing a theoretical discharge rate curve and the
 133 temporal scale at which each of the measurement definitions apply. IER = Instantaneous effusion rate; TADR
 134 = time-averaged discharge rate (weekly, daily); ER = eruption rate; MOR = mean output rate, t_0 = eruption
 135 start time; t_{stop} = eruption stop time.

136

137

138 At the beginning of many basaltic fissure eruptions, the discharge rate increases rapidly to a
 139 maximum value, then gradually drops to lower values as the eruption proceeds and the feeder
 140 dike empties (Wadge, 1981). This behaviour has been observed and documented at several basaltic
 141 effusive eruptions and on different volcanoes, such as Etna and Stromboli (Italy), Fogo (Cape
 142 Verde), Holhuraun (Iceland), Piton de la Fournaise (La Réunion), Kilauea (Hawaii), (Hon et al.,
 143 1994; Calvari et al., 2005, 2018; Harris et al., 2005a, 2011, 2012; Lodato et al., 2007; Spampinato et al.,
 144 2008a, 2008b; Ganci et al., 2012a, 2013, 2018; Cappello et al., 2016; Coppola et al., 2017; Patrick et al.,
 145 2017; Pedersen et al., 2017). The general trend of declining discharge rate is overlapped by a local
 146 variability giving rise to pulses of the order of hours along the lava flow channel (Lautze et al.,
 147 2004; Bailey et al., 2005; Harris et al., 2005b), that reflect more frequent pulses occurring at the main
 148 vent (James et al., 2007). High effusion rate has been related to a greater crystal content of the lava
 149 (up to 70%), whereas it apparently has no effect on lava porosity, which is uniformly decreasing

150 with distance from the vent (Soldati et al., 2018). An important parameter affecting lava flow
151 emplacement speed is the roughness of the topographic surface on which the flow is spreading,
152 with greater roughness increasing flow brecciation and favouring the change from pahoehoe to aa
153 (Rumpf et al., 2018).

154

155 3. Lava Flows and Lava Flow Fields

156 Many lava flows are divisible into smaller lava bodies, or flow units, each of which has a top
157 which cooled and solidified before another flow unit superposed on it (Walker, 1971). A lava flow
158 field or compound lava flow is a lava body divisible into flow units (Figure 3) produced by a
159 single vent or fissure during an uninterrupted period of effusion (Walker, 1971; Kilburn, 1996).
160 Superposed flow units in a compound flow are separated by an interval of time ranging from
161 minutes to more than a year (Walker, 1971).



162

163 **Figure 3** - Aerial view of the active complex lava flow field during Stromboli's 2002-03 flank eruption,
164 showing several vents (red) feeding several flow units displaying both pahoehoe and aa surfaces. Photo by
165 INGV.

166

167 Effusive volcanic eruptions form either single lava flow units or compound lava flow fields,
168 depending on the eruption duration: short-lived effusive pulses form single lava flows, also
169 defined as volume-limited lava flows (Guest et al., 1987), whereas long-lasting eruptions promote
170 the emplacement of complex lava flow fields (Kilburn & Lopes 1988, 1991; Calvari and Pinkerton,
171 1998; Calvari et al., 2005, 2010, 2018; Patrick et al., 2017; Pedersen et al., 2017). A flow may generate
172 major new lava streams by bifurcation, breaching and overflow of vents, channels, or tubes.
173 Bifurcation is controlled by topography and is a random process, breaching and overflows are
174 cooling controlled and more systematic (Kilburn & Lopes, 1988). Thus, the growth pattern of a lava
175 flow field may follow comparable cooling trends beneath the randomizing effect of bifurcation
176 (Kilburn & Lopes, 1988). A simple evolutionary sequence starts with lava flow field widening until
177 an equilibrium width is reached, followed by flow lengthening until inhibited by its crust (Kilburn
178 & Lopes, 1988). With further crustal growth, flow thickening starts at the front and migrates
179 upstream, leading to maintained thickening, breaching or overflow (Kilburn & Lopes, 1988;
180 Kilburn & Guest, 1993). The development of lava tubes may significantly modify this general
181 model, promoting longer flows than the channel-fed equivalent (Calvari & Pinkerton, 1998;
182 Kauahikaua et al., 1998).

183

184 Walker (1971) observed that whether a flow is compound or simple seems to be determined
185 primarily by the rate of extrusion of lava at the surface, with a low rate favouring the formation of
186 compound flows, and a high rate producing simple flows. In addition, the rate of extrusion also
187 influences the morphology of lava flows, with aa surfaces forming in conditions of high IER, and
188 pahoehoe flows forming at low IER (Griffiths & Fink, 1992a, 1992b; Lyman et al., 2005; Cashman et
189 al., 2006).

190

191 The hazards posed by a single lava flow unit and by a compound lava flow field are extremely
192 different as are their sizes. A compound lava flow field usually has a larger surface area than a
193 single flow unit. In addition, compound lava flow fields often comprise lava tubes, which increase
194 even more the possibility of lava to travel longer distances (Calvari & Pinkerton, 1998, 1999;
195 Kauahikaua et al., 1998). Long lasting eruptions fed by lava tubes develop on the flow field surface
196 several structures like tumuli, pressure ridges, inflation clefts, ephemeral vents, skylights,
197 toothpaste flows, squeeze-outs (Walker, 1991). All these features suggest low emplacement rate,
198 and conditions of a slowly expanding lava flow field with low hazard.

199

200 4. Sheet Flows

201 Sheet flows are characterised by flat surfaces and are common during the initial phases of an
202 eruption, when IER is high and the flow spreads laterally from the vent inundating the
203 surrounding topography (Figures 4A and B, Figure 5; Ballard et al., 1979; Lipman & Banks, 1987;
204 Kilburn & Guest, 1993; Hon et al., 1994; Calvari et al., 2005). At this stage, lava channel
205 development is inhibited by the high IER, that can reach values as high as $180 \text{ m}^3 \text{ s}^{-1}$ (1989 Etna
206 eruption; Bertagnini et al., 1990), $280 \text{ m}^3 \text{ s}^{-1}$ (2002-03 Stromboli eruption; Calvari et al., 2005), 350 m^3
207 s^{-1} (2014-15 Holuhraun eruption; Pedersen et al., 2017), or even $980 \text{ m}^3 \text{ s}^{-1}$ (20 August 2011 Etna
208 paroxysm; Behncke et al., 2014). A flow front consisting of sheet lava is often diagnostic of high
209 advance rate, and it is possible to judge whether a flow was in a fast-advance regime based simply
210 on a quick look at the flow front morphology (Patrick et al., 2017). Sheet flow front advance rates
211 of up to 2 km/day (0.023 m s^{-1} ; Table 1) have been measured during the 1991-1993 eruption at Mt
212 Etna on aa lava flows (Calvari et al., 1994); up to 500 m/day (0.006 m s^{-1} ; Table 1) during the 2014-
213 2015 Pahoehoe effusive crisis at Kilauea on pahoehoe flows (Poland et al., 2016); and of 50 km/h
214 (13.889 m s^{-1} ; Table 1) during the initial phases of the 1951 O Shima eruption (Japan; Mason &
215 Foster, 1953). Sheet flows normally do not contain lava channels or lava tubes because they appear
216 to be conditioned by the combination of a flat topography and a high output rate (Lipman &
217 Banks, 1987; Hon et al., 1994). However, long-lived pahoehoe sheet flows comprising multiple
218 inflated lobes (Figure 4C) propagate downslope as a series of interconnected lobes that eventually
219 can develop lava tubes (Hon et al., 1994). Sheet flows normally last 1-2 days during the initial
220 phases of an eruption (Lipman & Banks, 1987), and tend to develop a convex upward upper
221 surface when slowly moving, and a nearly flat upper surface when rapidly advancing (Lipman &
222 Banks, 1987). The hazard posed by sheet flow expansion is very high because the spread fast, but it
223 is normally limited to the few first days of an eruption. Inflated pahoehoe sheet flows instead
224 advance more slowly, and can be distinguished by their fast counterpart because they display a
225 different top surface, where initial individual flow lobes can still be distinguished (Figure 4C).



226
227 **Figure 4** - (A) Example of a sheet flow with aa surface overflowing the rim of the South-East Crater during
228 the initial phases of Etna's 1989 eruption. (B) Aa sheet flow spreading during the 2002-03 Etna's flank
229 eruption (foreground), while the eruptive fissure was producing lava fountains and ash plume
230 (background). Photo by INGV. (C) Pahoehoe inflated sheet flow, Kilauea, where individual flow lobes can
231 still be distinguished.

232



233
234 **Figure 5** - Cinder cone formed along the 2001 eruptive fissure, south flank of Mt. Etna, in 2001, with initial
235 volume-limited sheet flows (at the two sides of the channel), and in the middle the main lava channel
236 bounded by multiple levées. Photo by INGV.

237

238

239 5. Levées

240 When a lava flow spreads along a surface, cooling results in the development of regions of
241 stationary liquid at its margins, called levées (Figure 6A; Hulme, 1974). Sparks et al. (1976)
242 described four different types of levées: initial, accretionary, rubble and overflow. Initial levées are
243 formed in active lava flows by the stagnation and cooling of lava at the margins of an initial flow
244 unit (Figure 5; Hulme, 1974; Sparks et al., 1976), and are characterized by a broad zone of marginal
245 clinker bounding the central flowing plug. Effectively these are the rubbly flanks of the aa flow left
246 behind after the initial flow passed through (Lipman & Banks 1987). Narrowing of the actively
247 flowing central zone results in inward growth of the initial levées, an effect observed in the
248 morphologies of Etna's proximal channel levées (Figure 5; Bailey et al., 2006). Initial levées
249 determine channel width, and their sizes depend on slope (Sparks et al., 1976). Accretionary levées

250 are slowly built up by smearing of the hot, ductile clinkers onto the sides and tops of the levées,
251 welding together to form a solid levée (Sparks et al., 1976). Formation of aa clinker at the flow
252 margins by shearing and milling results in piles of clinker being gradually piled up at the margins
253 of the flow zone (Naranjo et al., 1992). This process is responsible for rubble levées (Sparks et al.,
254 1976) that overlie the inner edge of the initial levée. Rubble levées are laid down by the initial flow
255 front passage (Sparks et al. 1976) and may later become overprinted with overflow levées (e.g.,
256 Lipman & Banks, 1987; Naranjo et al., 1992; Bailey et al., 2006). Overflow or accretionary levées are
257 emplaced during periods of increased effusion rate, when flux exceeds channel capacity, causing
258 the channel to overflow for a short period of time (Kilburn & Guest, 1993; Bailey et al., 2006). An
259 additional type of levée is called "swollen levées", and occurs when channel lava laterally intrudes
260 the levée causing swelling, brecciation and local lava extrusion (Kilburn & Guest, 1993). Similarly,
261 "seeps" of viscous spiny or toothpaste pahoehoe have been observed as extruded from shield
262 flanks or from perched lava channels (Patrick & Orr, 2012). Active levées become static levées
263 when they become strong enough to withstand pressure from the channelled lava, or when lateral
264 pressure on the margins is removed by draining of the channel, and a static levée may become
265 active if material accumulating in the channel increases the pressure exerted on the levées (Guest
266 et al., 1987). During waning flow, levées become accreted to the inner walls of the channel
267 (Naranjo et al., 1992), and nested levées may form (Lipman & Banks 1987). Continued narrowing
268 of the central flow zone can leave a series of abandoned rubble levées that attest to sustained
269 inward levée growth. An additional type of levées has been observed at Stromboli, and called
270 "excavated debris levées" (Figure 6B; Calvari et al., 2005) because the lava spreading on the steep
271 Sciara del Fuoco slope has excavated downward and pushed laterally the cold and loose debris,
272 thus improving channel formation. These levées can be distinguished from the other types by their
273 lower temperature (Calvari et al., 2005).



274
275 **Figure 6 -** (A) Lava channel, about 30 m wide and 20 m deep, formed in aa flow during the 2001 Etna's flank
276 eruption, bounded by high levées. Note the person with blue jacket in the middle of the channel for scale. (B)
277 Active lava channel during the 2007 Stromboli's flank eruption, with "excavated debris levées" (light brown)
278 around the vent and uppermost channel. The width of the vent is about 6 m.

279

280

281 6. Lava Channels

282 Lava flows are non-Newtonian or Bingham fluids, and as soon as a lava flow stabilises, it develops
283 a channel zone. Thus the channel is a zone of flowing lava contained between static levées (Sparks
284 et al., 1976; Lipman & Banks 1987; Kilburn & Guest 1993; Soldati et al., 2018). Channel formation
285 results from an increase in flow surface velocity in the axial zone of a flow, with the velocity
286 gradient between the rapidly moving central area and the stagnating margins becoming greater
287 with time and eventually abrupt, and is marked by an initial channel generally much wider than in
288 the stable channel zone (Lipman & Banks, 1987). This process is normally quite fast (at Mauna Loa
289 in 1984; Lipman & Banks, 1987), and lava may start spreading within channels just a few hours (at
290 Mt. Etna in 1991; Calvari et al., 1994; Calvari & Pinkerton 1998) or 24 h after the eruption start (at
291 Holuhraun in 2014; Pedersen et al., 2017). Lipman & Banks (1987) have classically described the
292 architecture of channel-fed lava flow systems, recognising four zones down a channel-fed lava
293 flow: (1) a proximal, stable channel zone where levées are well-developed and mostly static
294 (Figure 6); (2) a medial, transitional channel zone, where the flow is channelized and bounded by
295 incipient rubble levées still deformable; (3) a distal dispersed flow zone, where there are no levées
296 and the lava is moving across its entire width; and (4) the flow front or flow toe, where the system

297 is still spreading and expanding. The channel propagates downslope along the transitional and
298 dispersed flow zones, where there are no levées present and the flow core is covered by breccia all
299 the way to the flow front (Soldati et al., 2018). This change confined a progressively greater volume
300 of faster moving lava to a smaller channel cross section in an upstream direction, until the surface
301 of the central area became more incandescent and finally consisted dominantly of fluid lava
302 (Lipman & Banks, 1987). Lava channels develop as a consequence of cooling, which forms as soon
303 as a crust develops, thick enough to prevent lateral flow (Hulme, 1974). Following Hulme (1974),
304 the time needed to form this crust is proportional to the fourth power of the flow depth, and thus
305 time increases rapidly with increasing depth of flow.

306 Pre-existing topography affects the form of the channel network in different ways, depending if
307 we are dealing with aa or pahoehoe flows. At Mauna Loa, Dietterich & Cashman (2014) found that
308 steeper slopes correspond to higher braiding indices on pahoehoe flows, whereas Soldati et al.
309 (2018) at Piton de la Fournaise described structures of the aa channel network varying with
310 distance from vent rather than with time, with single channels forming on steeper slopes and
311 braided channels on shallower slopes. Soldati et al. (2018) observed that changes in the
312 architecture of the aa flow are reversible because the flow can switch back and forth between
313 single and braided channel configurations multiple times during its emplacement. In addition,
314 Soldati et al. (2018) recognise the importance of flow rate on lava flow structures, with lava flows
315 characterized by low effusion rates more prone to braiding compared to high effusion rate flows
316 on any given slope. Channel networks govern the distribution of lava supply within a flow,
317 because changes in the channel topography can dramatically alter the effective volumetric flux in
318 any one branch, which affects both flow length and advance rate (Dietterich & Cashman, 2014).
319 Specifically, branching will slow and shorten flows, while merging can accelerate and lengthen
320 them (Dietterich & Cashman, 2014), with important effects on lava flow hazard evaluation.
321 Consideration of channel networks is thus important for predicting lava flow behaviour and
322 possibly mitigating flow hazards with diversion barriers.

323

324 7. Lava Tubes

325 A lava tube is a roofed conduit through which molten lava travels away from its vent (Figure 7;
326 Kauahikaua et al., 1998). Lava tubes normally form during long-lasting eruptions in both
327 pahoehoe and aa lava flow fields (Kilburn & Guest, 1993; Calvari & Pinkerton, 1998). At Etna,
328 Calvari & Pinkerton (1998) described a minimum time of 4 days in order to form a tube sector

329 within channelled aa lava flows, and considered a steady magma discharge rate as the main
330 requirement for tube formation. In turn, the discharge rate defines the size of the tube, with longer
331 and wider tubes being formed by higher discharge rates. Calvari & Pinkerton (1998) describe tube
332 formations at Etna within aa lava flows in conditions of discharge rate spanning three orders of
333 magnitude. By contrary, lava tubes within pahoehoe flows described in Hawaii apparently form
334 only in a restricted and low range of discharge rate (1 to 5 m³ s⁻¹, Peterson et al., 1994). At
335 Nyiragongo during the 2002 flank eruption lava tubes transporting lava within lake Kivu
336 apparently formed along the arterial flow in less than a week (Komorowski et al., 2003), although
337 it appears from the description that lava surface cooling was favoured by the contact with the lake
338 water. At Kilauea, Hon et al. (1994) describe the process of lava tube formation within pahoehoe
339 sheet flows in absence of lava channels and as a gradual concentration of the hot flow interior,
340 with the flow margins cooling within hours after emplacement by edge effect, developing
341 preferential pathways along which lava tubes will gradually develop. Lava tubes within pahoehoe
342 sheet flows begin to form after 2-4 weeks of their emplacement, but information about this process
343 are scant because normally, being formed on low topographic gradient, they do not drain and
344 therefore are difficult to observe (Hon et al., 1994). Lava tubes formed within pahoehoe sheet flows
345 have been observed to develop with time an equidimensional section, whereas immature tubes
346 (less than 1 week old) have widths more than one order of magnitude greater than their height
347 (Hon et al., 1994; Kauahikaua et al., 1998).



348
349 **Figure 7** - (A) Skylight above an aa master lava tube formed during the 2014-15 eruption of Fogo volcano,
350 Cape Verde. Note the smooth pahoehoe slabs bounding the topographic surface and inner skylight walls

351 resulting from late tube drainage. (B) Skylight above an active lava tube emplaced within pahoehoe inflated
352 sheet flows, Kilauea volcano, Hawaii. Note the gas clouds from skylights that reveal the tube path.

353

354

355 Four processes have been recognised by which lava channels evolve into tubes: (i) inward growth
356 of channel crust, rooted to flow margins; (ii) repeated overflow and accretion causing levées to
357 arch and seal over channels; (iii) jamming of crustal fragments on the channel surface; (iv) and
358 wholesale attachment of a complete channel crust to the bounding levées (Peterson & Swanson
359 1974; Greeley, 1987; Kilburn & Guest, 1993; Calvari & Pinkerton 1998; Kauahikaua et al., 1998).

360 Broad, flat pahoehoe sheet flows evolve into elongated tumuli with an axial crack as the flanks of
361 the original flow were progressively buried by breakouts (Kauahikaua et al., 1998). Sometimes, the
362 tubes began to thermally erode the floor (downcutting), frequently observed through skylights,
363 with rates of 10 cm/day (Kauahikaua et al., 1998). This process increases the insulation of tubes
364 making them increasingly deeper and more difficult to detect. Lava streams normally occupy only
365 a small fraction of the tube interior, and the stream has a free surface that is primarily gravity-
366 driven (Kauahikaua et al., 1998).

367

368 The presence of lava tubes within an active lava flow field is very important for hazard assessment
369 because their insulation can allow lava to flow farther from the vent. In fact, a cooling of just
370 $\sim 1^\circ\text{C}/\text{km}$ has been estimated for the lava flowing inside a lava tube (Calvari et al., 1994; Keszthelyi
371 1995; Kauahikaua et al., 1998; Heltz et al., 2003). Tubes allow lava to travel for longer distances
372 than when flowing within channels, threatening areas very distant from the active vent. The effect
373 of lava tubes is thus similar to the downslope displacement of the effusive vent. This is the reason
374 why the most devastating lava flow fields have involved the formation of extensive lava tube
375 networks (Calvari & Pinkerton, 1998; Kauahikaua et al., 1998; Crisci et al., 2003; Branca et al., 2013;
376 Patrick et al., 2017; Pedersen et al., 2017; Calvari et al., 2018; Soldati et al., 2018).

377

378 8. Hazard implications

379 One of the more challenging aspects for predicting lava flow dynamics is that the rheological
380 properties of lava flows evolve during eruption and emplacement as a consequence of cooling,
381 degassing and crystallization. This produces strongly heterogeneous flow conditions, with lava
382 textures and morphologies that evolve both in space and time (Kolzenburg et al., 2017). The

383 evolution of the lava's rheology determines, for instance, whether lava advances as sheet- or
384 channel-like flows, and also dictates its surface morphology, which in turn has great influence on
385 heat loss from the flow (Kolzenburg et al., 2017). In addition to changes in rheology, lava surface
386 morphology changes also as a result of climaxing or declining discharge rate. Thus, as an eruption
387 proceeds, we normally observe a first phase displaying the formation of sheet flows when the
388 discharge rate is high and the flow is still free to expand laterally invading the topography that
389 surrounds the effusive vent. This phase normally lasts from one to a few days. This stage
390 corresponds to a great hazard for the areas surrounding the vent, especially because lava can reach
391 high speeds (Table 1), but the hazard is limited in time.

392

393 A second stage corresponds to the formation of levées and one or more well-defined channels,
394 confining the lava within well-established paths and driving it more efficiently to longer distances
395 from the vent. This stage can last from weeks to years, and the greatest hazard is located at the
396 frontal zone, where the flow has not yet established its path and is free to expand laterally.
397 However, sudden changes in the supply rate, or upstream blockages formation and removal, can
398 result in sudden and even large channel overflows that may invade the area around the channel.
399 Overflows are normally short-lived, but their damage can be potentially devastating.

400

401 The hazard posed by the expanding frontal zone, being it increasingly far away from the vent, is
402 also increasingly lower due to its decreasing speed of expansion, a result of cooling and crust
403 formation. This stage normally offers enough time to evacuate buildings or infrastructures
404 avoiding loss of life. With time, and if magma supply is steady enough, lava tubes may develop
405 within the lava flow field (Calvari & Pinkerton, 1998; Kauahikaua et al., 1998). The insulating effect
406 of lava tubes allow lava to travel longer distances from the main vent, increasing the possibility of
407 inflation or endogenous growth of the lava flow field (Hon et al., 1994; Calvari & Pinkerton, 1998),
408 and resulting in increased hazard for the distal portion of the lava flow field, where breakouts can
409 suddenly open giving rise to fast spreading secondary flows (Calvari et al., 1994, 2018). In
410 addition, an underestimated hazard derives from the reactivation of lava flow fronts due to the
411 overlapping of two or more lava flow units when the lower/earlier has not yet solidified, thus
412 allowing a combination of the molten core of the two overlapped flows (Applegarth et al., 2010).

413

414 Each country with frequently erupting volcanoes has developed proper systems to face volcanic
415 crises, depending on the most common lava flow morphologies, speeds and features. At Kilauea
416 volcano, where an effusive eruption is going on since 1983, the scientists of the Hawaiian Volcano
417 Observatory (HVO) in charge of volcano monitoring and hazard assessment produce lava flow
418 maps including potential flow paths based on topographic steepest-descent calculations (e.g.,
419 Kauahikaua & Tilling, 2014; Poland et al., 2016; Neal et al., 2018). This is enough to forecast the
420 possible expansion of lava, given that pahoehoe lava flows can be very fast, change rapidly
421 directions following minor topography changes, and cause a reversal topography due to inflation
422 (Hon et al., 1994).

423

424 By contrast on Etna, where frequent effusive eruptions normally occur every few years (Harris et
425 al., 2011, 2012; Bonaccorso & Calvari, 2013), satellite measurements of IER (Ganci et al., 2011,
426 2012b) are crucial during the initial phases of an eruption (Bonaccorso et al., 2015). These are used
427 at first to estimate the maximum distance that a single flow unit can travel (Calvari & Pinkerton,
428 1998; Wright et al., 2001; Bonaccorso et al., 2015), and in the meanwhile the same parameters are
429 used to run lava flow simulations using cellular automata models, that provide a more accurate
430 and reliable forecast of lava flow expansion (Crisci et al., 2003; Vicari et al., 2011; Ganci et al.,
431 2012b; Del Negro et al., 2013) as well as a probabilistic modelling of future eruptions (Cappello et
432 al. 2011, 2012, 2013). However, the discovery that lava tubes develop and grow even within aa lava
433 flow fields typical of Etna (Calvari & Pinkerton, 1998; 1999) has revealed an important hazard that
434 must be considered when dealing with long-lived effusive eruptions having a steady supply
435 (Calvari et al., 1994; Calvari & Pinkerton, 1998; Solana et al., 2017; Calvari et al., 2018). Reliable
436 tube growth simulations are not available at the moment, and all we can do when lava tube
437 presence has been detected within growing lava flow fields is to run lava flow simulation moving
438 the effusive vents where new breakouts open at the end of the tube path (Cappello et al., 2016;
439 Neal et al., 2018).

440

441 **9. Concluding remarks**

442 The analysis of lava flow morphology can help evaluate the possible hazard posed by active lava
443 flows and lava flow fields, because each lava type forms in different phases of an eruption and in
444 different conditions of discharge rate, lava rheology and topography. The initial stages of effusive
445 eruptions normally involve the highest rates of effusion (Wadge 1981; Harris et al., 2011, 2012),

446 rapidly declining to a lower value and steady state when the feeder dike stabilizes and drain.
447 Thus, the initial phases of effusive eruptions at highest flow rate normally produce sheet flows,
448 where a thin sheet of lava spreads laterally at high speed (Table 1) around the vent (Pedersen et al.,
449 2017). Although very hazardous, they normally last few hours to days, and are followed by aa lava
450 flows spreading at still high discharge rates. These soon form channels, whose levées protect the
451 villages and infrastructures located at the two sides, but at this stage it is still possible that
452 overflows from the main channel may invade properties and land (Neal et al., 2018). When
453 discharge rate declines, earlier aa flows may be covered by slower pahoehoe flows. If we can
454 measure the IER during an effusive eruption, we can apply the simple formula proposed by
455 Walker (1971) that relates IER and maximum flow length, in order to estimate a priori the
456 maximum distance that a single flow unit can reach from its vent, as has been done on Etna using
457 Walker's formula appropriately modified for Etna's lava (Calvari & Pinkerton, 1998; Wright et al.,
458 2001; Bonaccorso et al., 2015; Solana et al., 2017). If instead the first flows forming at high rates are
459 pahoehoe, then we can apply the expertise of HVO and produce a map with lines of maximum
460 steepness of the ground, in a way to forecast the path followed by pahoehoe lobes and inflated
461 pahoehoe sheet flows (Kauahikaua & Tilling, 2014; Poland et al., 2016; Neal et al., 2018). If the
462 eruption proceeds, and a complex lava flow field forms, it is possible to run appropriate models
463 simulating lava flow emplacement (Crisci et al., 2003; Cappello et al., 2011, 2016; Ganci et al., 2011,
464 2012b; Vicari et al., 2011). However, we must take into account that complex and long-lived lava
465 flow fields may promote the formation of hidden lava tubes, which allow the lava to expand with
466 very little heat loss and spread further downslope than when travelling free on the surface or
467 within channels (Calvari & Pinkerton, 1998; Kauahikaua et al., 1998; Calvari et al., 2018). Because
468 no reliable models exist at the moment for simulating the effect of lava tubes, the only possibility
469 to evaluate lava flow invasion in these cases is to apply existing lava flow models to any new
470 major breakouts opening at the edge of the lava flow field (e.g., Cappello et al., 2016).
471 Identification of inflated zones of the lava flow field and of potential ephemeral vent sites in its
472 distal regions is critical for hazard assessment because they allow flows to lengthen significantly
473 over their calculated cooling-limited lengths (Pinkerton & Sparks 1976; Calvari & Pinkerton, 1998).
474 In all conditions, the possibility to extract useful lava flow parameters from satellite images may
475 help when ground measurements are impossible or dangerous (Ganci et al., 2011, 2012a, 2012b,
476 2013, 2018; Cappello et al., 2016).

477 The experience gained at well monitored volcanoes can be applied to those cases where a
478 monitoring system is not well developed or is lacking, and the analysis of lava flow morphology
479 can help evaluating the hazard when and where there is no possibility to obtain reliable lava flow
480 mapping and effusion rate measurements from ground or remote sensing techniques. This was the
481 case for example of the 2014-15 eruption at Fogo volcano (Cape Verde), or the 2002 Nyiragongo
482 eruption (Komorowski et al., 2003; Cappello et al., 2016; Calvari et al., 2018).

483

484

485 **Acknowledgements**

486 I would like to thank the Editor Ciro Del Negro for handling the manuscript, Jim Kauahikaua for
487 his precious and valuable revision and suggestions that significantly improved the paper, Steve
488 Conway for the correction of the English style, and an anonymous reviewer for his/her comments.

489

490 **References**

- 491 Applegarth L. J., Pinkerton H., James M. R., Calvari S. (2010) - Lava flow superposition: the reactivation of
492 flow units in compound flow fields. *Journal of Volcanology and Geothermal Research*, 194, 100-106,
493 doi: 10.1016/j.jvolgeores.2010.05.001.
- 494 Bailey J.E., Harris A.J.L., Dehn J., Calvari S., Rowland S.K. (2006) – The changing morphology of an open
495 lava channel on Mt. Etna. *Bulletin of Volcanology*, DOI 10.1007/s00445-005-0025-6, 68, 6, 497-515.
- 496 Ballard, R.D., Holcomb R.T., and van Andel T.H. (1979) - The Galapagos Rift at 86°W: 3. Sheet Flows,
497 Collapse Pits, and Lava Lakes of the Rift Valley. *Journal of Geophysical Research*, 84, B10, 5407-5422.
- 498 Behncke B., Branca S., Corsaro R. A., De Beni E., Miraglia L., Proietti C. (2014) - The 2011–2012 summit
499 activity of Mount Etna: Birth, growth and products of the new SE crater. *Journal of Volcanology and*
500 *Geothermal Research* 270, 10–21, <http://dx.doi.org/10.1016/j.jvolgeores.2013.11.012>
- 501 Bertagnini A., Calvari S., Coltelli M., Landi P., Pompilio M. and Scribano V. (1990) - The 1989 eruptive
502 sequence. In "Mt. Etna: the 1989 eruption", Barberi F., Bertagnini A., Landi P. Eds., CNR-GNV Special
503 Issue, Giardini, Pisa, 10-22.
- 504 Bonaccorso A., Calvari S. (2013) - Major effusive eruptions and recent lava fountains: Balance between
505 erupted and expected magma volumes at Etna volcano. *Geophysical Research Letters*, 40, 6069-6073,
506 doi:10.1002/2013GL058291.
- 507 Bonaccorso A., Calvari S., Boschi E. (2015) - Hazard mitigation and crisis management during major flank
508 eruptions at Etna volcano: reporting on real experience. In: Harris, A.J.L., De Groot, T., Garel, F., &
509 Carn, S.A. (Editors) "Detecting, Modelling and Responding to Effusive Eruptions", Geological Society,

510 London, Special Publications (IAVCEI) Series, vol. 426, pp. 447-461, <http://doi.org/10.1144/SP426.4>,
511 ISBN 978-1-86239-736-1.

512 Branca S., De Beni, E., Proietti C. (2013) - The large and destructive 1669 AD eruption at Etna volcano:
513 reconstruction of the lava flow field evolution and effusion rate trend. *Bull. Volcanol.*, 75:694, doi:
514 10.1007/s00445-013-0694-5.

515 Calvari S., Coltelli M., Neri M., Pompilio M. and Scribano V. (1994) - The 1991-93 Etna eruption: chronology
516 and lava flow field evolution, *Acta Vulcanologica*, 4, 1-14.

517 Calvari S., Ganci G., Silva Victória S., Hernandez P. A., Perez N. M., Barrancos J., Alfama V., Dionis S.,
518 Cabral J., Cardoso N., Fernandes P., Melian G., Pereira J.M., Semedo H., Padilla G., and Rodriguez F.
519 (2018) - Satellite and Ground Remote Sensing Techniques to Trace the Hidden Growth of a Lava Flow
520 Field: The 2014–2015 Effusive Eruption at Fogo Volcano (Cape Verde). *Remote Sensing*, 10, 1115,
521 doi:10.3390/rs10071115.

522 Calvari S., Lodato L., Steffke A., Cristaldi A., Harris A.J.L., Spampinato L., Boschi E. (2010) – The 2007
523 Stromboli flank eruption: chronology of the events, and effusion rate measurements from thermal
524 images and satellite data. *Journal Geophysical Research, Solid Earth*, 115, B4, B04201,
525 doi:10.1029/2009JB006478.

526 Calvari S. and H. Pinkerton (1998) - Formation of lava tubes and extensive flow field during the 1991-93
527 eruption of Mount Etna, *Journal of Geophysical Research*, 103 (B11), 27291-27302.

528 Calvari S. and Pinkerton H. (1999) Lava tube morphology on Etna and evidence for lava flow emplacement
529 mechanisms. *Journal of Volcanology and Geothermal Research*, 90, 263-280.

530 Calvari S., Spampinato L., Lodato L., Harris A.J.L., Patrick M.R., Dehn J., Burton M.R., Andronico D. (2005) –
531 Chronology and complex volcanic processes during the 2002-2003 flank eruption at Stromboli volcano
532 (Italy) reconstructed from direct observations and surveys with a handheld thermal camera. *Journal of*
533 *Geophysical Research*, 110, B02201, doi:10.1029/2004JB003129.

534 Cappello, A., Vicari, A., Del Negro, C. (2011) - Retrospective validation of a lava-flow hazard map for Mount
535 Etna volcano. *Annals of Geophysics*, 54, 634–640, <http://doi.org/10.4401/ag-5345>.

536 Cappello, A., Neri, M., Acocella, V., Gallo, G., Vicari, A., Del Negro, C. (2012) - Spatial vent opening
537 probability map of Etna volcano (Sicily, Italy). *Bulletin of Volcanology*, 74, 2083–2094, [http://doi.org/](http://doi.org/10.1007/s00445-012-0647-4)
538 [10.1007/s00445-012-0647-4](http://doi.org/10.1007/s00445-012-0647-4).

539 Cappello, A., Bilotta, G., Neri, M., Del Negro, C. (2013) - Probabilistic modelling of future volcanic eruptions
540 at Mount Etna. *Journal of Geophysical Research: Solid Earth*, 118, 1925–1935, [http://doi.org/10.1002/](http://doi.org/10.1002/jgrb.50190)
541 [jgrb.50190](http://doi.org/10.1002/jgrb.50190).

542 Cappello, A., G. Ganci, S. Calvari, N. M. Pérez, P. A. Hernández, S. V. Silva, J. Cabral, and C. Del Negro
543 (2016), Lava flow hazard modeling during the 2014–2015 Fogo eruption, Cape Verde, *J. Geophys. Res.*
544 *Solid Earth*, 121, doi:10.1002/2015JB012666.

545 Cashman, K. V., Kerr, R.C., and Griffiths, R.W. (2006) A laboratory model of surface crust formation and
546 disruption on lava flows through non-uniform channels. *Bulletin of Volcanology* 68, (DOI
547 10.1007/s00445-005-0048-z): 753-770.

548 Cashman K.V., Thornber C., Kauahikaua J.P. (1999) - Cooling and crystallization of lava in open channels,
549 and the transition of Pāhoehoe Lava to 'A'ā. *Bull Volcanol* (1999) 61:306–323.

550 Coltelli M., Marsella M., Proietti C., Scifoni S. (2012) - The case of the 1981 eruption of Mount Etna: An
551 example of very fast moving lava flows. *Geochemistry, Geophysics, Geosystems*, 13:1, Q01004,
552 doi:10.1029/2011GC003876.

553 Coppola D., Di Muro A., Peltier A., Villeneuve N., Ferrazzini V., Favalli M., Bachèlery P., Gurioli L., Harris
554 A.J.L., Moune S., Vlastélic I., Galle B., Arellano S., Aiuppa A. (2017) - Shallow system rejuvenation
555 and magma discharge trends at Piton de la Fournaise volcano (La Réunion Island). *Earth and
556 Planetary Science Letters*, 463, 13-24, <http://dx.doi.org/10.1016/j.epsl.2017.01.024>.

557 Crisci G.M., Di Gregorio S., Rongo R., Scarpelli M., Spataro W., and Calvari S. (2003) – Revisiting the 1669
558 Etnean eruptive crisis using a cellular automata model and implications for volcanic hazard in the
559 Catania area. *Journal of Volcanology and Geothermal Research*, 123, 1/2, 211-230.

560 Del Negro, C., Cappello, A., Neri, M., Bilotta, G., Hérault, A. & Ganci, G. (2013) - Lava flow hazards at
561 Mount Etna: constraints imposed by eruptive history and numerical simulations. *Scientific Reports*, 3,
562 3493, <http://doi.org/10.1038/srep03493>.

563 Dietterich HR, Cashman KV (2014) Channel networks within lava flows: formation, evolution, and
564 implications for flow behavior. *J Geophys Res Earth Surf* 119(8):1704–1724. [https://doi.org/10.1002/
565 2014JF003103](https://doi.org/10.1002/2014JF003103).

566 Favalli, M., A. Fornaciai, F. Mazzarini, A. Harris, M. Neri, B. Behncke, M. T. Pareschi, S. Tarquini, and E.
567 Boschi (2010), Evolution of an active lava flow field using a multitemporal LIDAR acquisition, *J.
568 Geophys. Res.*, 115, B11203, doi:10.1029/2010JB007463.

569 Finch, R. H., and Macdonald, G. A. (1953). *A Contribution to General Geology - Hawaiian Volcanoes during
570 1950*. U.S. Geological Survey Bulletin 996-B, 27-89.

571 Ganci G, Cappello A, Bilotta G, Hérault A, Zago V and Del Negro C (2018) Mapping Volcanic Deposits of
572 the 2011–2015 Etna Eruptive Events Using Satellite Remote Sensing. *Front. Earth Sci.* 6:83. doi:
573 10.3389/feart.2018.00083.

574 Ganci, G., James, M. R., Calvari, S., and Del Negro, C. (2013). Separating the thermal fingerprints of lava
575 flows and simultaneous lava fountaining using ground-based thermal camera and SEVIRI
576 measurements. *Geophys. Res. Lett.* 40, 5058–5063. doi: 10.1002/grl.50983.

577 Ganci, G., Harris, A. J. L., Del Negro, C., Guehenneux, Y., Cappello, A., Labazuy, P., et al. (2012a). A year of
578 lava fountaining at Etna: volumes from SEVIRI. *Geophys. Res. Lett.* 39:L06305. doi:
579 10.1029/2012GL051026.

580 Ganci, G., Vicari, A., Cappello, A., Del Negro, C. (2012b) - An emergent strategy for volcano hazard
581 assessment: From thermal satellite monitoring to lava flow modelling. *Remote Sensing of*
582 *Environment*, 119, 197–207.

583 Ganci, G., Vicari, A., Fortuna L., Del Negro, C. (2011) - The HOTSAT volcano monitoring system based on
584 combined use of SEVIRI and MODIS multispectral data. *Annals of Geophysics*, 54, 5, doi: 10.4401/ag-
585 5338.

586 Giordano D., and Russell J.K. (2018) - Towards a structural model for the viscosity of geological melts. *Earth*
587 *and Planetary Science Letters*, 501, 202-212, <https://doi.org/10.1016/j.epsl.2018.08.031>.

588 Greeley R. (1987) - The Role of Lava Tubes in Hawaiian Volcanoes. U.S.G.S. Prof. Paper 1350, 2, 1589-1606.

589 Griffiths, R. W. and J. H. Fink (1992a). Solidification and Morphology of Submarine Lavas: A Dependence on
590 Extrusion Rate. *JOURNAL OF GEOPHYSICAL RESEARCH* 97(B13): 19729-19737.

591 Griffiths, R. W. and J. H. Fink (1992b). The Morphology of Lava Flows in Planetary Environments:
592 Predictions From Analog Experiments. *JOURNAL OF GEOPHYSICAL RESEARCH* 97(B13): 19739-
593 19748.

594 Guest, J.E.; Underwood, J.R.; Greeley, R. (1980) - Role of lava tubes in flows from the Observatory Vent, 1971
595 eruption on Mount Etna. *Geol. Mag.* 117, 601-606.

596 Guest J.E., Kilburn C.R.J., Pinkerton H., and Duncan A.M. (1987) - The evolution of lava flow-fields:
597 observations of the 1981 and 1983 eruptions of Mount Etna, Sicily. *Bull. Volc.*, 49:527-540.

598 Guilbaud, M.-N., Self S., Thordarson T., Blake S. (2005) - Morphology, surface structures, and emplacement
599 of lavas produced by Laki, A.D. 1783–1784. *Geol. Soc. Am. Special Paper* 396, 81-102, doi: 10.1130/
600 2005.2396(07).

601 Harris A.J.L., Dehn J., and Calvari S. (2007a) - Lava effusion rate definition and measurement: a review. *Bull.*
602 *Volc.*, 70:1-22, doi: 10.1007/s00445-007-0120-y.

603 Harris, A. J. L., J. Dehn, M. R. James, C. Hamilton, R. Herd, L. Lodato, and A. Steffke (2007b), Pāhoehoe
604 flow cooling, discharge, and coverage rates from thermal image chronometry, *Geophys. Res. Lett.*, 34,
605 L19303, doi:10.1029/2007GL030791.

606 Harris, A. J. L., J. Dehn, M. Patrick, S. Calvari, M. Ripepe, L. Lodato (2005a), Lava effusion rates from hand-
607 held thermal infrared imagery: an example from the June 2003 effusive activity at Stromboli, *Bull.*
608 *Volcanol.*, 68, 107-117, doi: 10.1007/s00445-005-0425-7.

609 Harris A.J.L., Belousov A., Calvari S., Delgado-Granados H., Hort M., Koga K., Mei E.T.W., Harijoko A.,
610 Pacheco J., Prival J.-M., Solana C., Thordarson T., Thouret J.-C., van Wyk de Vries B. (2017a) -
611 Translations of volcanological terms: cross-cultural standards for teaching, communication, and
612 reporting, *Bulletin of Volcanology*, 79:57, doi: 10.1007/s00445-017-1141-9.

613 Harris A., Dehn J., Patrick M., Calvari S., Ripepe M., Lodato L. (2005b) – Lava effusion rates from hand-held
614 thermal infrared imagery: an example from the June 2003 effusive activity at Stromboli. *Bulletin of*
615 *Volcanology*, d.o.i.: 10.1007/s00445-005-0425-7, 68, 107-117.

616 Harris, A.J.L., Rowland S.K., Villeneuve N., Thordarson T. (2017b) - Pāhoehoe, ‘a’ā, and block lava: an
617 illustrated history of the nomenclature. *Bull Volcanol* 79: 7, doi:10.1007/s00445-016-1075-7.

618 Harris A.J.L., Steffke A., Calvari S., Spampinato L. (2011) - Thirty years of satellite-derived lava discharge
619 rates at Etna: Implications for steady volumetric output. *Journal of Geophysical Research*, 116, B08204,
620 doi: 10.1029/2011JB008237.

621 Harris A.J.L., Steffke A., Calvari S., Spampinato L. (2012) – Correction to “Thirty years of satellite-derived
622 lava discharge rates at Etna: Implications for steady volumetric output”. *Journal of Geophysical*
623 *Research-Solid Earth*, 117, B08207, doi:10.1029/2012JB009431.

624 Helz, R. T., Heliker, C., Hon, K., and Mangan, M. (2003) - Thermal efficiency of lava tubes in the Puu O'o-
625 Kupaianaha eruption. U.S.G.S. Professional Paper 1676: 105-120.

626 Hon, K.; Kauahikaua, J.; Denlinger, R.; Mackay K. (1994) - Emplacement and inflation of pahoehoe sheet
627 flows: Observations and measurements of active lava flows on Kilauea Volcano, Hawaii. *Geol. Soc.*
628 *Am. Bull.* 106, 351-370.

629 Hulme G. (1974) - The interpretation of lava flow morphology. *Geophysical Journal of Royal Astronomic*
630 *Society* 39: 361-383.

631 James, M. R., L. J. Applegarth and H. Pinkerton, (2012), Lava channel roofing, overflows, breaches and
632 switching: insights from the 2008–2009 eruption of Mt. Etna, *Bull. Volcanol.*, 74: 107-117, doi:
633 10.1007/s00445-011-0513-9.

634 James, M. R., H. Pinkerton, and L. J. Applegarth (2009), Detecting the development of active lava flow fields
635 with a very-long-range terrestrial laser scanner and thermal imagery, *Geophys. Res. Lett.*, 36, L22305,
636 doi:10.1029/2009GL040701.

637 James, M. R., H. Pinkerton, and S. Robson (2007), Image-based measurement of flux variation in distal
638 regions of active lava flows, *Geochem. Geophys. Geosyst.*, 8, Q03006, doi:10.1029/2006GC001448.

639 James, M. R., H. Pinkerton, and M. Ripepe (2010), Imaging short period variations in lava flux, *Bull.*
640 *Volcanol.*, 72, 671–676, doi:10.1007/ s00445-010-0354-y.

641 Kauahikaua, J., Cashman, K.V., Mattox, T.N., Heliker, C.C., Hon, K.A., Mangan, M.T., Thornber, C.R., 1998.
642 Observations on basaltic lava streams in tubes from Kīlauea Vol- cano, island of Hawai'i. *J. Geophys.*
643 *Res.* 103:27,303–27,323. <http://dx.doi.org/10.1029/97JB03576>.

644 Kauahikaua, J., Sherrod D.R., Cashman, K.V., Heliker, C.C., Hon, K.A., Mattox, T.N., Johnson J.A. 2003.
645 Hawaiian Lava-Flow Dynamics During the Pu‘u ‘Ö‘ö- Kūpaianaha Eruption: A Tale of Two Decades.
646 U.S.G.S. Prof. Pap. 1676, 63-88.

647 Kauahikaua J.P., and Tilling R.I. (2014) - Natural Hazards and Risk Reduction in Hawai'i. U.S. Geological
648 Survey Professional Paper 1801, 397-427.

649 Keszthelyi, L. (1995), A preliminary thermal budget for lava tubes on the Earth and planets, *Journal of*
650 *Geophys. Res.*, 100(B10), 20,411–20,420.

651 Keszthelyi, L., and R. Denlinger (1996), The initial cooling of pahoehoe flow lobes, *Bull. Volcanol.*, 58, 5–18.

652 Kilburn CRJ (1996) Patterns and Predictability in the Emplacement of Subaerial Lava Flows and Flow Fields.
653 In: Scarpa R and Tilling R (Eds) *Monitoring and Mitigation of Volcano Hazards*. 491-540, Springer
654 ISBN-13: 978-3-642-80089-4 , doi: 10.1007/978-3-642-80087-0.

655 Kilburn CRJ (1981) Pahoehoe and Aa lavas: A Discussion and Continuation of the Model of Peterson and
656 Tilling. *Journal of Volcanology and Geothermal Research*, 11, 373-382.

657 Kilburn CRJ, Guest JE (1993) Aa lavas of Mount Etna, Sicily. In: *Active lavas* (UCL Press, London), p 73–106.

658 Kilburn C.R.J. and Lopes R.M.C. (1988) - The growth of aa lava flow fields on Mount Etna, Sicily. *Jour.*
659 *Geoph. Res.*, 93(B12):14,759-14,772.

660 Kilburn C.R.J. and Lopes R.M.C. (1991) - General Patterns of Flow Field Growth: Aa and Blocky Lavas. *Jour.*
661 *Geoph. Res.*, 96(B12):19,721-19,732.

662 Kolzenburg, S., Giordano D., Thordarson T., Hoskuldsson A., Dingwell D.B. (2017) - The rheological
663 evolution of the 2014/2015 eruption at Holuhraun, central Iceland. *Bull Volcanol* (2017) 79: 45, doi:
664 10.1007/s00445-017-1128-6.

665 Komorowski J.-C., Tedesco D., Kasereka M., et al. (2003) - The January 2002 Flank Eruption of Nyiragongo
666 Volcano (Democratic Republic of Congo): Chronology, Evidence for a Tectonic Rift Trigger, and
667 Impact of Lava Flows on the City of Goma. *Acta Vulcanologica*, 15(1-2), 27-62.

668 Lautze, N. C., A. J. L. Harris, J. Bailey, M. Ripepe, S. Calvari, J. Dehn, S. Rowland, and K. Evans - Jones
669 (2004), Evidence for pulsed magma supply at Mount Etna during 2001, *J. Volcanol. Geotherm. Res.*,
670 137, 231–246.

671 Lipman, P. W., and N. G. Banks (1987), 'A'a flow dynamics, Mauna Loa 1984, in *Volcanism in Hawaii*, U.S.
672 *Geol. Surv. Prof. Pap.*, 1350, 1527–1567.

673 Lodato L., Spampinato L., Harris A.J.L., Calvari S., Dehn J., and Patrick M. (2007) - The Morphology and
674 Evolution of the Stromboli 2002-03 Lava Flow Field: An Example of Basaltic Flow Field Emplaced on a
675 Steep Slope. *Bulletin of Volcanology*, DOI 10.1007/s00445-006-0101-6, 69, 661-679.

676 Lyman, A. W., Kerr, R.C., and Griffiths, R.W. (2005). Effects of internal rheology and surface cooling on the
677 emplacement of lava flows. *JOURNAL OF GEOPHYSICAL RESEARCH* 110(B08207,
678 doi:10.1029/2005JB003643)

679 Mason A.C., Foster H.L. (1953) - Diversion of lava flows at O Shima, Japan. *American Journal of Science*, 251,
680 249-258.

681 Mattox, T.N., Heliker, C., Kauahikaua, J., Hon, K. (1993) Development of the 1990 Kalapana Flow Field,
682 Kilauea Volcano, Hawaii. *Bull. Volcanol.* 55, 407-413.

683 Macdonald G.A. (1962) - The 1959 and 1960 eruptions of Kilauea volcano, Hawaii, and the construction of
684 walls to restrict the spread of the lava flows. *Bulletin Volcanologique* 24(1): 249-294.

685 Naranjo JA, Sparks RSJ, Stasiuk MV, Moreno H, Ablay GJ (1992) Morphological, structural and textural
686 variations in the 1988–1990 andesite lava of Lonqimay volcano, Chile. *Geol Mag* 129:657–678.

687 Neal CA, Brantley SR, Antolik L, et al. (2018), The 2018 rift eruption and summit collapse of Kilauea
688 Volcano. *Science*, doi: 10.1126/science.aav7046.

689 Patrick M., and Orr T. (2012) - Rootless shield and perched lava pond collapses at Kilauea Volcano, Hawai'i.
690 *Bulletin of Volcanology* 74 : 67–78, doi: 10.1007/s00445-011-0505-9.

691 Patrick M., Orr T., Fisher G., Trusdell F., and Kauahikaua J. (2017) - Thermal mapping of a pāhoehoe lava
692 flow, Kilauea Volcano. *Journal of Volcanology and Geothermal Research* 332 (2017) 71–87,
693 <http://dx.doi.org/10.1016/j.jvolgeores.2016.12.007>.

694 Pedersen G.B.M., Höskuldsson A., Dürig T., Thordarson T., Jónsdóttir I., Riishuus M.S., Óskarsson B.V.,
695 Dumont S., Magnusson E., Gudmundsson M.T., Sigmundsson F., Drouin V.J.P.B., Gallagher C.,
696 Askew R., Gudnason J., Moreland W.M., Nikkola P., Reynolds H.I., Schmith J., and the IES eruption
697 team (2017) - Lava field evolution and emplacement dynamics of the 2014–2015 basaltic fissure
698 eruption at Holuhraun, Iceland. *Jour. Volc. Geoth. Res.*, 340, 155-169.

699 Peterson, D.W., R.T. Holcomb, R.I. Tilling, and R.L. Christiansen, 1994, Development of lava tubes in the
700 light of observations at Mauna Ulu, Kilauea Volcano, Hawaii, *Bull. Volcanol.*, 56, 343-360.

701 Peterson D.W., and Swanson D.A. (1974) - Observed formation of lava tubes during 1970-1971 at Kilauea
702 volcano, Hawaii. *Studies in Speleology*, 2, 209-222.

703 Peterson D.W. and Tilling R.I. (1980) - Transition of basaltic lava from pahoehoe to aa, Kilauea Volcano,
704 Hawaii: field observations and key factors. *Journal of Volcanology and Geothermal Research*, 7, 271-
705 293.

706 Pinkerton H, Sparks RSJ (1976) The 1975 sub-terminal lavas, Mount Etna: a case history of the formation of a
707 compound lava field. *J Volcanol Geotherm Res* 1(2):167–182

708 Poland, M. P., Orr, T.R., Kauahikaua, J., Brantley, S.R., Babb, J.L., Patrick, M.R., Neal, C.A., Anderson, K.R.,
709 Antolik, L., Burgess, M., Elias, T., Fuke, S., Fukunaga, P., Johanson, I.A., Kagimoto, M., Kamibayashi,
710 K., Lee, L., Miklius, A., Million, W., Moniz, C., Okubo, P.G., Sutton, A.J., Takahashi, T.J., Thelen, W.A.,
711 Tollett, W., Trusdell, F.A. (2016). The 2014–2015 Pāhoa lava flow crisis at Kilauea Volcano, Hawai'i:
712 Disaster avoided and lessons learned. *GSA Today* 26(2): 4-10.

713 Rhéty, M., A. Harris, N. Villeneuve, L. Gurioli, E. Médard, O. Chevrel, and P. Bachélery (2017), A
714 comparison of cooling-limited and volume-limited flow systems: Examples from channels in the Piton

715 de la Fournaise April 2007 lava-flow field, *Geochem. Geophys. Geosyst.*, 18, 3270–3291, doi:10.1002/
716 2017GC006839.

717 Rumpf M.E., Lev E., Wysicki R. (2018) - The influence of topographic roughness on lava flow emplacement.
718 *Bull. Volcanol.*, 80:63, <https://doi.org/10.1007/s00445-018-1238-9>.

719 Solana, M.C., Calvari S., Kilburn, C.R.J., Gutierrez H., Chester D., Duncan A. (2017) Supporting the
720 Development of Procedures for Communications During Volcanic Emergencies: Lessons Learnt from
721 the Canary Islands (Spain) and Etna and Stromboli (Italy). In: *Advances in Volcanology, Observing
722 the Volcano World, Volcano Crisis Communication*, Eds: Fearnley C.J., Bird D.K., Haynes K., McGuire
723 W.J., and Jolly G., Springer Open, 289-305, DOI: 10.1007/11157_2016_48. ISBN 978-3-319-44095-8, ISSN
724 2364-3285 (electronic), <https://doi.org/10.1007/978-3-319-44097-2>.

725 Soldati A., Harris A.J.L., Gurioli L., Villeneuve N., Rhéty M., Gomez F., Whittington A. (2018) - Textural,
726 thermal, and topographic constraints on lava flow system structure: the December 2010 eruption of
727 Piton de la Fournaise. *Bulletin of Volcanology*, 80:74, <https://doi.org/10.1007/s00445-018-1246-9>.

728 Spampinato L., Calvari S., Harris A.J.L., Dehn J., (2008a) – Evolution of the lava flow field. In: “THE
729 STROMBOLI VOLCANO: An integrated study of the 2002-2003 Eruption”, *American Geophysical
730 Union Monograph Series*, Calvari S., Inguaggiato S., Puglisi G., Ripepe M. and Rosi M. (Editors), v.
731 182, 201-212, doi: 101029/182GM17. ISBN 978-0-87590-447-0.

732 Spampinato L., Calvari S., Oppenheimer C., Lodato L. (2008b) - Shallow magma transport for the 2002-03
733 Mt. Etna eruption inferred from thermal infrared surveys. *Journal of Volcanology and Geothermal
734 Research*, 177, 301-312, doi:10.1016/j.jvolgeores.2008.05.013.

735 Sparks RSJ, Pinkerton H, Hulme G (1976) Classification and formation of lava levees on Mount Etna, Sicily.
736 *Geology* 4:269– 271.

737 Thordarson, T., and Self, S. (1993) - The Laki (Skaftar Fires) and Grimsvotn eruptions in 1783-1785. *Bull.
738 Volcanol.*, 55, 233-263.

739 Vicari, A., Bilotta, G. Bonfiglio, S., Cappello, A., Ganci, G., Hérault, A., Rustico, E., Gallo, G., Del Negro, C.
740 (2011) - LAV@HAZARD: a web-GIS interface for volcanic hazard assessment. *Annals of Geophysics*,
741 54, 662–670, <http://doi.org/10.4401/ag-5347>.

742 Wadge G. (1981) - The variation of magma discharge during basaltic eruptions. *Jour. Volc. Geoth. Res.*, 11:
743 139-168.

744 Walker G.P.L. (1971) - Compound and Simple Lava Flows and Flood Basalts. *Bull Volc.*, 35(2):579-590.

745 Walker, G. P. L. (1973), Lengths of lava flows, *Philos. Trans. R. Soc. London, Ser. A*, 274, 107–118.

746 Walker, G.P.L. (1991) - Structure, and origin by injection under surface crust, of tumuli, “lava rises,” “lava-
747 rise pits,” and “lava inflation clefts” in Hawaii. *Bull. Volcanol.* 53, 546– 58.

748 Wright, R., Flynn, L. P., Harris, A. J. L. (2001) Evolution of lava flow-fields at Mount Etna, 27–28 October
749 1999, observed by Landsat 7 ETM. *Bulletin of Volcanology*, 63, 1 – 7, <http://doi.org/10.1007/s00445>
750 0100124.